Design and performance simulation of a molecular Doppler wind lidar

Fahua Shen (沈法华)[1*], Hyunki Cha[2], Jihui Dong (董吉辉)[1], Dukhyeon Kim[3], Dongsong Sun (孙东松)[1], and Sung Ok Kwon[2]

[1]*Anhui Institute of Optics and Fine Mechanics, Chinese Academy of Sciences, Hefei 230031, China*

[2]*Korea Atomic Energy Research Institute, Daejeon, 305-353, Korea*

[3]*Hanbat National University, Daejeon, 305-719, Korea*

[*]*E-mail: sfh81914@tom.com*

Received October 30, 2008

A mobile molecular Doppler wind lidar at an eye-safe wavelength of 355 nm based on double-edge technique is being built in Hefei (China) for wind measurement from 10-to 40-km altitude. The structure of this lidar system is described. A triple Fabry-Perot etalon is employed as a frequency discriminator whose parameters are optimized. The receiver system is designed to achieve compactness and stability by putting in a standard 19-inch socket bench. Simulation results show that within the wind speed dynamic range of ±100 m/s, the horizontal wind errors due to noise are less than 1 m/s below 20-km altitude for 100-m vertical resolution, and less than 5.5 m/s from 20 km up to 40 km for 500-m vertical resolution with 400-mJ laser energy, 30-min temporal resolution, and a 45-cm aperture telescope.

OCIS codes: 120.0120, 140.0140, 280.0280.

doi: 10.3788/COL20090707.0593.

Wind measurements from ground and airborne platforms provide data which are important to the mesoscale dynamic process, transport and exchange in the atmosphere[1−3]. A Mie Doppler wind lidar has been already successfully developed at Anhui Institute of Optics and Fine Mechanics, Chinese Academy of Sciences. This aerosol-based wind lidar can only be used for wind measurement in low troposphere where the aerosol backscattering is high[4,5]. For the high altitude where the aerosol concentration is extremely low, this kind of lidar is useless. Fortunately, molecule is a dependable and reasonably uniform source on a global basis. This offers the feasibility for wind measurements from the high troposphere up to stratosphere by using molecular backscattering and is very important for airborne-based wind measurements[6−9]. For the purpose of wind measurement at high altitude, a mobile Doppler wind lidar based on molecular backscattering is being built in Hefei, China. This system uses an air-spaced Fabry-Perot (FP) etalon as a frequency discriminator, and the etalon aperture is divided into three channels, two edge channels and one locking channel. The design parameters of this triple FP etalon are optimized for measuring Doppler shift based on Rayleigh backscattering. The receiver system including FP etalon, optics components, detectors, and processing software has been developed. The designed receiver is very compact and stable. Doppler lidar with this kind of receiver may become commercial in the near future.

Contrast to the narrow aerosol backscattered spectrum, the molecular backscattered spectrum is broadened widely by the random motion of the air molecules. The molecular-based double-edge technique uses two edge channels of the triple etalon located in the wings of the broadened molecular backscattered spectrum to determine the Doppler shift, as shown in Fig. 1(a). The locking channel of the etalon is used to measure the outgoing laser frequency and lock the etalon to the laser frequency for a high accuracy wind measurement.

The configuration of the triple etalon is shown in Fig. 1(b). The cavity lengths are slightly different by optically coating one of the edge channels and the locking channel. As this structure keeps the difference of the cavity length constant, the transmission properties of the etalons will have a stable profile during cavity tuning or fluctuation. This etalon has a nominal cavity spacing of 12.5 mm and an effective finesse of 7. Its cavity scan range is more than 0.4 μm. All the parameters of the etalon are optimized and the optimizing procedure will be described specifically in another paper. The transmission function for a real FP etalon at a given frequency ν can be derived as the integration of the Airy function over the incident beam divergence angle θ[10]:

$$h(\nu) = \frac{2}{\theta_0^2}\int_0^{\theta_0} \frac{T_{\rm p}\theta {\rm d}\theta}{1+4\left(\frac{\nu_{\rm FSR}}{\pi\Delta\nu_{1/2}}\right)^2 \sin^2\left(\frac{\pi\nu\cos\ \theta}{\nu_{\rm FSR}}\right)}, \qquad (1)$$

where $T_{\rm p}$, $\Delta\nu_{1/2}$, $\nu_{\rm FSR}$, θ_0 are the peak transmission, the full-width at half-maximum (FWHM) of the etalon, the free spectral range, and the beam divergence angle, respectively.

The normalized Mie-and Rayleigh-scattering spectral functions, $f_{\rm M}(\nu)$ and $f_{\rm R}(\nu,{\rm T})$, respectively, have Gaussian profile that are given by

$$f_{\rm M}(\nu) = (1/\pi\Delta\nu_l^2)^{1/2}\exp(-\nu^2/\Delta\nu_l^2), \qquad (2)$$

$$f_{\rm R}(\nu,T) = \int_{-\infty}^{+\infty} f_{\rm M}(\nu-\nu')G_{\rm R}(\nu',T){\rm d}\nu', \qquad (3)$$

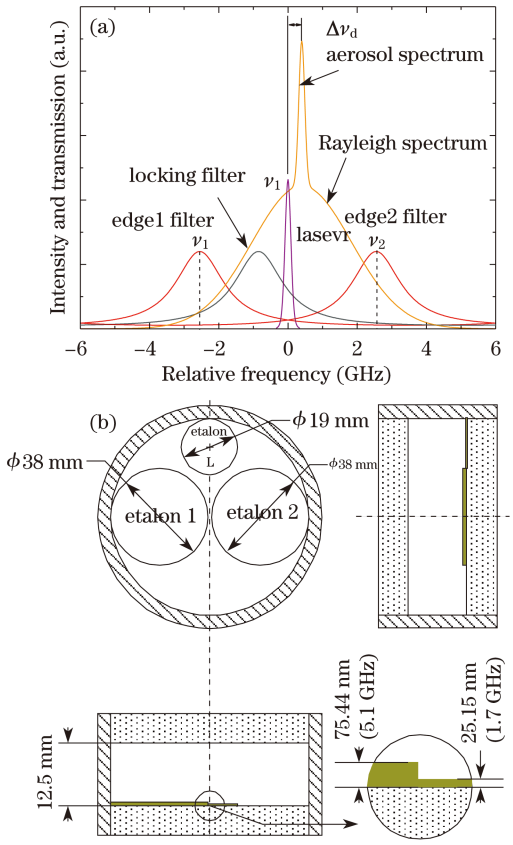

Fig. 1. (a) Spectra profiles of Rayleigh and Mie scattering signals along with transmission functions of three filters; (b) configuration of the triple FP etalon.

where $\Delta\nu_l$=$\delta\nu/(4\ln 2)^{1/2}$, $\delta\nu$ is the FWHM of the aerosol backscattering spectrum, which can be replaced by the FWHM of outgoing laser spectrum since the Brownian motion of aerosol particles does not broaden the spectrum significantly; $G_{\rm R}(\nu,T) = (1/\pi\Delta\nu_{\rm r}^2)^{1/2}\exp(-\nu^2/\Delta\nu_{\rm r}^2)$, $\Delta\nu_{\rm r} = (8kT/M\lambda^2)^{1/2}$ is the 1/e width of the atmospheric molecular spectrum, k is the Boltzmann constant, T is the temperature, M is the average mass of an atmospheric molecule. Then, Mie scattering (or outgoing laser) transmittance and Rayleigh scattering transmittance at atmospheric temperature T can be written as

$$T_{\rm L}(\nu) = T_{\rm M}(\nu) = \int_{-\infty}^{+\infty} h(\nu-\nu')f_{\rm M}(\nu')\mathrm{d}\nu', \tag{4}$$

$$T_{\rm R}(\nu,T) = \int_{-\infty}^{+\infty} T_{\rm M}(\nu-\nu')G_{\rm R}(\nu',T)\mathrm{d}\nu'. \tag{5}$$

The locking channel transmittance of the outgoing laser can be measured by two analog photomultiplier tube (PMT) detectors:

$$T_{\rm L}(\nu_{\rm L}) = a_1 I_{\rm Ls}/I_{\rm Le}, \tag{6}$$

where a_1 is a constant, $I_{\rm Ls}$ is the transmitted signal measured on the locking channel and $I_{\rm Le}$ is the signal measured on the corresponding energy monitor channel.

Assuming that the intensities of the backscattered light beams incident on to two edge channels of the etalons are equal and the two detectors have the same sensitivity, the transmitted signals measured on the two edge channels are

$$I_1(\nu) = a_2\left[I_{\rm R}T_{\rm R1}(\nu,T) + I_{\rm M}T_{\rm M1}(\nu)\right], \tag{7}$$

$$I_2(\nu) = a_2\left[I_{\rm R}T_{\rm R2}(\nu,T) + I_{\rm M}T_{\rm M2}(\nu)\right], \tag{8}$$

where a_2 is a constant, $I_{\rm M}$ and $I_{\rm R}$ are the aerosol backscattered signal and the Rayleigh backscattered signal, respectively. Response function is introduced to detect the relative change in the transmitted signals due to frequency shift:

$$R(\nu) = I_1(\nu)/I_2(\nu) = N_1/N_2, \tag{9}$$

where N_1 and N_2 are photon counts in the edge channels received by photon counting detectors. Then the line of sight (LOS) wind speed can be retrieved by

$$V_{\rm r} = \frac{\lambda}{2}\Delta\nu_{\rm d} = \frac{\lambda}{2}\left[R^{-1}(\nu) - T_{\rm L}^{-1}(\nu_{\rm L})\right], \tag{10}$$

where $\Delta\nu_{\rm d}$ is the Doppler frequency shift, $R^{-1}(\nu)$ and $T_{\rm L}^{-1}(\nu)$ are the inverse functions of $R(\nu)$ and $T_{\rm L}(\nu)$, respectively, which are measured during system calibration before actual wind measurement.

The Doppler lidar is designed for wind measurement from Rayleigh backscattering, which could obtain the wind profile up to the stratosphere. The system consists of four major subsystems, which are the laser transmitter subsystem, the scanning telescope (transceiver) subsystem, the receiver subsystem, and the controlling subsystem, as shown in Fig. 2. The transmitter is an injection-seeded Nd:YAG laser (Continuum Model 9050), which produces the output laser beam at 355 nm to take advantage of the λ^{-4} dependence of the molecular backscattering. The transceiver optical system consists of a 45-cm aperture Cassegrain telescope and a matching azimuth-over-elevation scanner that can provide full hemispherical pointing. Most of the light from the transmitter is expanded by a 10× expander to compress the

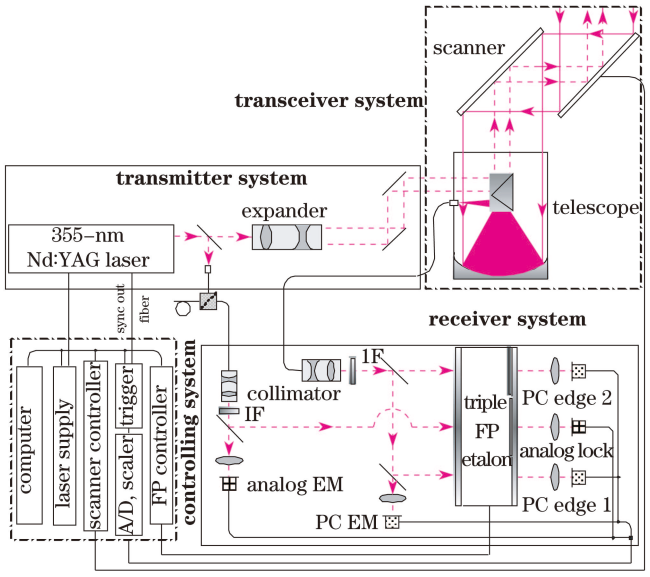

Fig. 2. Schematic diagram of Rayleigh Doppler lidar system. PC: photon counting; EM: energy monitor; A/D: analog-to-digital converter.

beam divergence to less than 0.1 mrad, and points to the atmosphere by the two-dimensional (2D) scanner. Then the backscattered signal that carries Doppler-shift information is collected and focused into a 200-μm-diameter multimode fiber to couple the signal from the telescope to the receiver. Before that, a very small fraction of the outgoing laser is coupled directly into the receiver through a 100-μm-diameter multimode fiber, and used as the reference signal to determine its frequency.

In the receiver, the reference light is coupled into a collimator to produce a collimated beam of 18-mm diameter. After passing through an interference filter (IF) with the bandwidth of 0.15 nm at 355 nm, the reference light is split into two channels by a beam splitter with a splitting ratio of R/T=23/77. The transmitted light illuminates the locking channel of the triple FP etalon (IC Extended ET70) which is used to sample the outgoing laser frequency as a reference. The backscattered light is coupled into another collimator to produce a collimated beam of 36-mm diameter. After passing through an IF, the backscattered light is split into three channels by a beam splitter and a beam splitting prism (BSP). Two of the light beams with 47% intensity for each are incident on to two edge channels of the etalon which provide the information used in the Doppler shift measurement. The other two beams with 23% of reference light and 6% of backscattered light serve as energy monitor channels to provide intensity normalization of the respective etalon channels during calibration. Each of the two reference-light channels is detected by a Hamamatsu PMT detector operated in analog mode (type: H5784-03) as the light is strong enough, while each of the three backscattered-light channels is detected by a Perkin Elmer photon counting mode channel photomultiplier (CPM) detector (type: MP943) for the very weak backscattered light. The laser operation, FP etalon spacing parallelism, data collection, and 2D scanner orientation are controlled by an industrial computer. Software is developed to achieve real-time signal processing and unattended operation. The system parameters are summarized in Table 1.

Table 1. Rayleigh Doppler Lidar System Parameters

	Parameter	Value
Transmitter	Wavelength	355 nm
	Laser Linewidth	200 MHz at 355 nm
	Laser Energy	400 mJ/pulse
	Laser Repetition Frequency	30 Hz
Transceiver	Telescope/Scanner Aperture	45 cm
	Field of View	0.2 mrad
	Optical Efficiency	$>85\%$
	Scan Range	$360^\circ\times90^\circ$
	Zenith Angle	30°
Receiver	Etalon Free Spectral Range	12 GHz
	Etalon FWHM	1.7 GHz
	Edge Channel Separation	5.1 GHz
	Locking Channel Separation	1.7 GHz
	Etalon Peak Transmission	60%
	CPM Quantum Efficiency	21%
	Filter Bandwidth	0.15 nm
	Filter Peak Transmission	$>40\%$

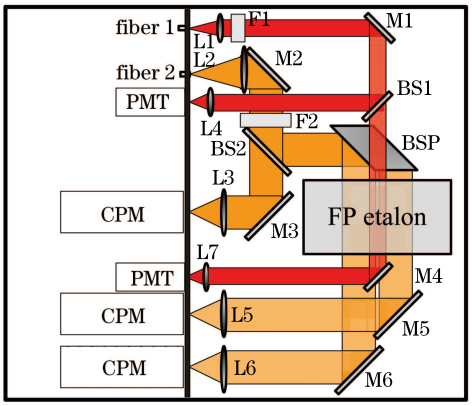

Fig. 3. Detailed configuration of the receiver system. M: mirror; L: lens; BS: beam splitter.

The designed receiver includes optics and detectors, and all of them are packaged in a room of 19×21 (inch), as shown in Fig. 3. As well known, the FP etalon central frequency is expected to drift under thermal changes, so the thermal stability nearby the FP etalon is of great importance to the wind measurement. Since the PMT detectors during work may become heaters, it is necessary to separate the FP etalon from the detectors. So the room is divided into two parts, one is for optical components and the other is for detectors and optical fiber sockets. In this receiver system, all optical parts are close to the FP etalon with minimized distance, therefore the receiver is compact, and the alignment is easy since most of optical components are attached to the etalon, and the system is stable because of the short optical arm. The detailed mechanical design is very complex and is not given here.

Wind velocity measurement sensitivity Θ is defined as a fractional change in the response function for 1-m/s wind velocity change and is given by

$$\Theta = \frac{1}{R}\frac{\partial R}{\partial V} = \frac{2}{\lambda}\frac{1}{R}\frac{\partial R}{\partial \nu}, \tag{11}$$

where R is the response function, V is the wind velocity, ν is the frequency.

As shown in Fig. 4, the velocity sensitivities of the designed triple etalon are nearly equal for the molecular and aerosol portions of the signal at atmospheric temperature of 210 K and slightly different as the temperature changes. In this case, the aerosol signal acts in a manner similar to the molecular signal. The sensitivity has a value of about 0.67%/(m/s) at the crossover point for the double-edge setup. By using 1976 USA standard atmospheric model and supposing the atmospheric temperature is exactly known, the line of sight (LOS) wind errors due to aerosol signal from 10- to 40-km altitude are calculated. As shown in Fig. 5, the induced errors for a LOS wind speed of 50 m/s are less than 0.06 m/s. While in practical data processing, the actual temperature profile may not be known exactly. If the estimated temperature

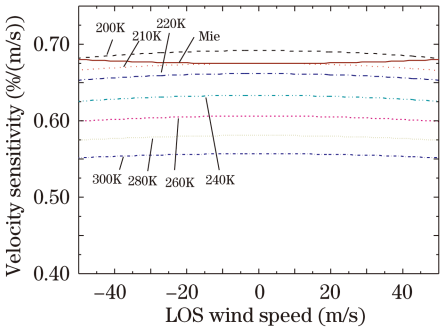

Fig. 4. Velocity sensitivities for molecular signal and aerosol signal versus LOS wind speed.

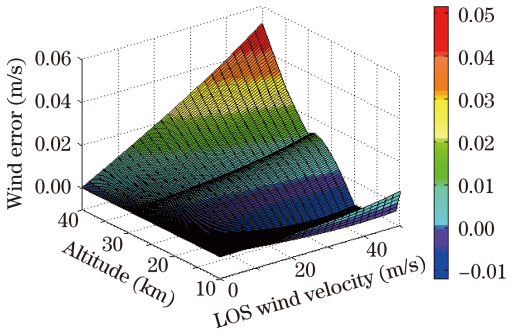

Fig. 5. LOS wind speed error caused by Mie signal.

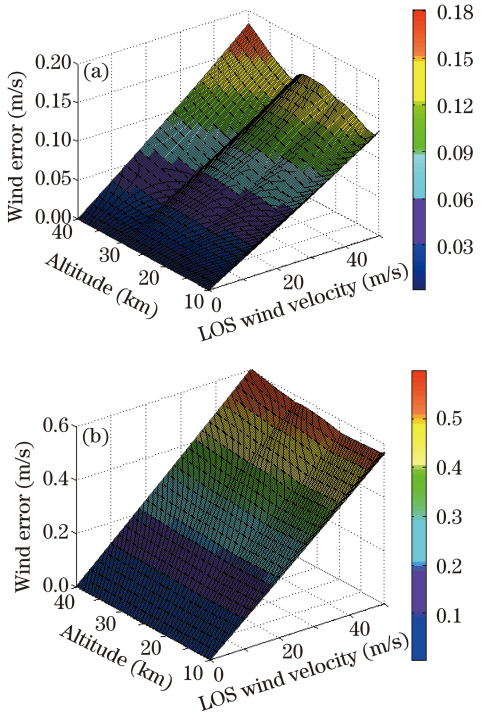

Fig. 6. LOS wind speed errors caused by temperature uncertainties of (a) 1 and (b) 5 K.

deviates from the actual value by 1 and 5 K, the LOS wind errors are below 0.18 and 0.6 m/s for a LOS wind speed of 50 m/s from 10-to 40-km altitude, respectively, as shown in Fig. 6. Then the relative errors on wind estimates due to temperature uncertainty are below 0.24%/K. So the accuracy in the temperature profile provided by the temperature model or other instruments such as Rayleigh lidar in the altitude sounded by the Doppler lidar should be much better than 5 K to determine the LOS wind speed profile with an acceptable accuracy. A new data processing method is proposed to reduce the temperature effects. During wind-retrieval processing, we define the temperature response function as $R_{\rm T}=(I_1+I_2)/I_{\rm E}$, where $I_{\rm E}$ is the signal measured on the corresponding energy monitor channel, to retrieve atmospheric temperature simultaneously. The detail of this method will be described elsewhere.

For outgoing laser frequency measurement, the measured light intensities are strong enough to allow us to ignore their statistical error. Then the statistical LOS wind speed error caused by detection noise is given as

$$\varepsilon_{\rm V}=1/({\rm SNR})\Theta, \tag{12}$$

where the signal-to-noise ratio (SNR) for ratio measurement of response function, is given as

$$({\rm SNR})=\left[({\rm SNR})_1^{-2}+({\rm SNR})_2^{-2}\right]^{-1/2}, \tag{13}$$

where $({\rm SNR})_1$ and $({\rm SNR})_2$ are the SNRs of the two edge channel signals. For estimating the statistical wind measurement error, shot noises associated with the measurement of two edge channel signals are assumed to be the dominant source. Meanwhile, the background in the edge channels is the sum of the detector dark counts and the solar background light. Then SNR for response function measurement can be given as

$${\rm SNR}_i=N_i/(N_i+N_{ib}+N_{\rm d})^{1/2}, \tag{14}$$

where i=1,2, N_i and N_{ib} are the sum of Rayleigh and Mie photon counts and the solar light photon counts collected by the detectors, respectively, $N_{\rm d}$ is the detector dark electron counts. Then adopting the 1976 USA standard atmospheric model, the LOS wind speed error can be simulated by using the parameters listed in Table 1 and Eqs. (11)−(14), as shown in Fig. 7. The temporal resolution is 6 min, the vertical resolution is 100 m for altitudes from 10 to 20 km and 500 m for altitudes above 20 km. LOS wind errors are below 0.5 m/s from 10 to 20 km, and below 3 m/s from 20 to 40 km.

To obtain the horizontal wind speed and direction, the laser beam is pointed to four directions of every 90° azimuth angle sequentially with a zenith angle of β and the first beam is pointed to the east. The LOS wind velocities are observed clockwise, namely

$$V_{\rm rk}=\frac{\lambda}{2}\left[R^{-1}(\nu_k)-T_{\rm L}^{-1}(\nu_{{\rm L}k})\right], k={\rm N,S,E,W}. \tag{15}$$

Defining east and north as positive directions, the zonal component and meridional component winds are determined as

$$V_x=\frac{V_{\rm rE}-V_{\rm rW}}{2\sin\beta}=\frac{(R_{\rm E}-R_{\rm W})}{(R_{\rm E}+R_{\rm W})}\frac{1}{\theta_{\rm V}\cdot\sin\beta}+\frac{\Delta V_{\rm EW}}{2\sin\beta}, \tag{16}$$

$$V_y=\frac{V_{\rm rN}-V_{\rm rS}}{2\sin\beta}=\frac{(R_{\rm N}-R_{\rm S})}{(R_{\rm N}+R_{\rm S})}\frac{1}{\theta_{\rm V}\cdot\sin\beta}+\frac{\Delta V_{\rm NS}}{2\sin\beta}, \tag{17}$$

where$\Delta V_{\rm EW}=[T_{\rm L}^{-1}(\nu_{\rm LW})-T_{\rm L}^{-1}(\nu_{\rm LE})]\cdot\lambda/2$, $\Delta V_{\rm NS}=[T_{\rm L}^{-1}(\nu_{\rm LS})-T_{\rm L}^{-1}(\nu_{\rm LN})]\cdot\lambda/2$, which are induced by outgoing laser frequency drifts. Then the horizontal wind velocity and direction are:

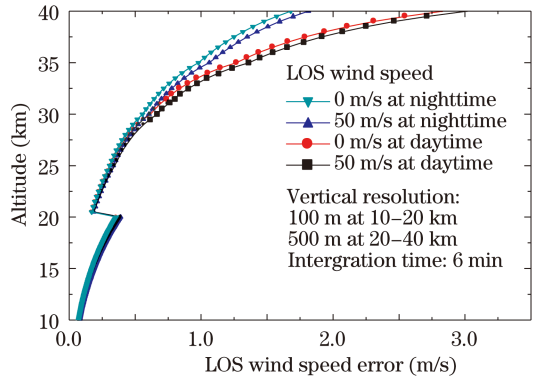

Fig. 7. LOS wind speed error versus altitude.

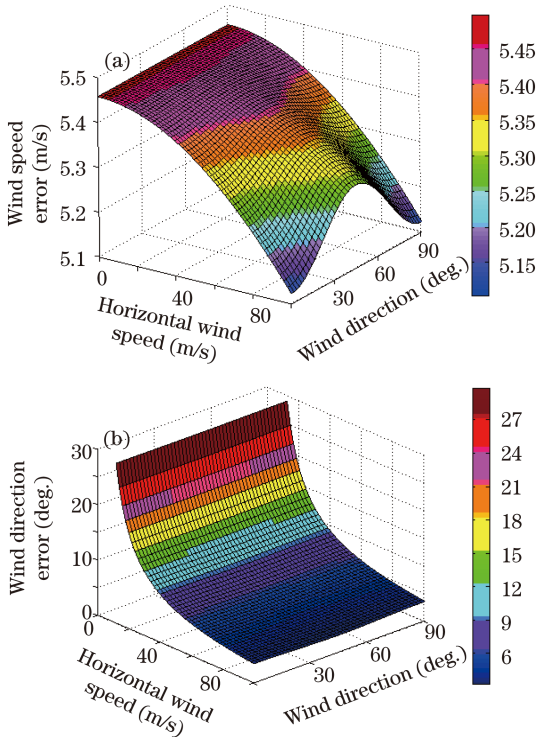

Fig. 8. Horizontal (a) wind speed and (b) direction errors at 40 km at daytime.

$$V_{\rm h} = \sqrt{V_x^2 + V_y^2}, \tag{18}$$

$$\varphi = \arctan(V_x/V_y) + \pi \left\{1 - \mathrm{sign}\left[(V_y + |V_y|) \cdot V_x\right]\right\}, \quad V_y \neq 0. \tag{19}$$

The angle of the wind direction is clockwise from the north. By using Eqs. (16)−(19), the errors in horizontal wind speed and direction can now be expressed as

$$\begin{aligned}\delta V_{\rm h} &= \left[(V_x/V_{\rm h})^2 \cdot (\delta V_x)^2 + (V_y/V_{\rm h})^2 \cdot (\delta V_y)^2\right]^{1/2} \\ &= \frac{1}{\theta_{\rm V} \sin\beta \cdot V_{\rm h}} \left[V_x^2 \cdot \left[\frac{2R_{\rm W}R_{\rm E}}{(R_{\rm E}+R_{\rm W})^2}\right]^2 \right. \\ &\times \sum_{i=1,2}\sum_{j={\rm E,W}} {\rm SNR}_{ij}^{-2} + V_y^2 \\ &\left. \times \left[\frac{2R_{\rm N}R_{\rm S}}{(R_{\rm N}+R_{\rm S})^2}\right]^2 \cdot \sum_{i=1,2}\sum_{j={\rm S,N}} {\rm SNR}_{ij}^{-2}\right]^{1/2}, \end{aligned} \tag{20}$$

$$\begin{aligned}\delta\varphi &= \left[\left(V_y/V_{\rm h}^2\right)^2 \cdot (\delta V_x)^2 + \left(V_x/V_{\rm h}^2\right)^2 \cdot (\delta V_y)^2\right]^{1/2} \\ &= \frac{1}{\theta_{\rm V} \sin\beta \cdot V_{\rm h}^2} \left[V_y^2 \cdot \left[\frac{2R_{\rm W}R_{\rm E}}{(R_{\rm E}+R_{\rm W})^2}\right]^2 \right. \\ &\times \sum_{i=1,2}\sum_{j={\rm E,W}} {\rm SNR}_{ij}^{-2} + V_x^2 \\ &\left. \times \left[\frac{2R_{\rm N}R_{\rm S}}{(R_{\rm N}+R_{\rm S})^2}\right]^2 \cdot \sum_{i=1,2}\sum_{j={\rm S,N}} {\rm SNR}_{ij}^{-2}\right]^{1/2}. \end{aligned} \tag{21}$$

Assume that the vertical resolution is 500 m and the integration time is 6 min for each LOS wind velocity measurement of the four cardinal directions, totally about 30 min per horizontal wind profile. The simulated horizontal wind speed and direction errors at 40 km are shown in Fig. 8. The results show that the speed error is below 5.5 m/s in the velocity dynamic range of ±100 m/s, the direction error is below 14° when the wind speed is larger than 25 m/s, and below 7° when the wind speed is larger than 50 m/s. From Fig. 5, the combined horizontal wind speed error at 20 km is about 1/6 of that at 40 km, so the speed error will below 1 m/s with 100-m vertical and 30-min temporal resolutions.

In conclusion, a triple FP etalon based Rayleigh Doppler wind lidar system is being built. The receiver subsystem has already been developed, which is very stable and compact and can be packaged in a room of 19×21 (inch). The simulation results show that taking 6-min integration time, the LOS wind speed accuracies are better than 0.5 m/s with 100-m vertical resolution below 20-km altitude, and better than 3 m/s with 500-m vertical resolution from 20 km up to 40 km. The accuracies of combined horizontal wind speed with a 30-min temporal resolution (30-min total time; 6 min for each cardinal direction) are better than 1 m/s below 20 km and 5.5 m/s from 20 km up to 40 km. The wind direction accuracies are associated with the magnitude of wind speed. They are better than 14° as the speed is larger than 25 m/s and better than 7° as the speed is larger than 50 m/s at 40 km. All the simulated results can meet the requirements of concerned applications.

This work was supported by the National "863" Project of China.

References

1. B. M. Gentry, H. Chen, and S. X. Li, Opt. Lett. **25,** 1231 (2000).
2. F. Shen, D. Sun, Z. Zhong, M. Chen, H. Xia, B. Wang, J. Dong, and X. Zhou, Acta Opt. Sin. (in Chinese) **26,** 1761 (2006).
3. L. Pu, J. Liu, and W. Chen, Acta Opt. Sin. (in Chinese) **27,** 379 (2007).
4. F. Shen, H. Cha, D. Sun, D. Kim, and S. O. Kwon, Opt. Rev. **15,** 204 (2008).
5. H. Xia, D. Sun, Y. Yang, F. Shen, J. Dong, and T. Kobayashi, Appl. Opt. **46,** 7120 (2007).
6. C. Flesia and C. L. Korb, Appl. Opt. **38,** 432 (1999).
7. C. Flesia, C. L. Korb, and C. Hirt, Opt. Lett. **25,** 1466 (2000).
8. J. Liu, L. Bu, J. Zhou, T. Yu, and W. Chen, Chinese J. Lasers (in Chinese) **33,** 1339 (2006).
9. J. Zhu, Y. Chen, Z. Yan, S. Wu, and Z. Liu, Chin. Opt. Lett. **6,** 449 (2008).
10. D. Hua, M. Uchida, and T. Kobayashi, Appl. Opt. **44,** 1305 (2005).